



HAL
open science

In-situ monitoring of changes in ultrastructure and mechanical properties of flax cell walls during controlled heat treatment

Elouan Guillou, Loïc Dumazert, Célia Caër, Alexandre Beigbeder, Pierre Ouagne, Gwenn Le Saout, Johnny Beaugrand, Alain Bourmaud, Nicolas Le Moigne

► To cite this version:

Elouan Guillou, Loïc Dumazert, Célia Caër, Alexandre Beigbeder, Pierre Ouagne, et al.. In-situ monitoring of changes in ultrastructure and mechanical properties of flax cell walls during controlled heat treatment. *Carbohydrate Polymers*, 2023, 321, pp.121253. 10.1016/j.carbpol.2023.121253 . hal-04180058

HAL Id: hal-04180058

<https://imt-mines-ales.hal.science/hal-04180058>

Submitted on 1 Sep 2023

HAL is a multi-disciplinary open access archive for the deposit and dissemination of scientific research documents, whether they are published or not. The documents may come from teaching and research institutions in France or abroad, or from public or private research centers.

L'archive ouverte pluridisciplinaire **HAL**, est destinée au dépôt et à la diffusion de documents scientifiques de niveau recherche, publiés ou non, émanant des établissements d'enseignement et de recherche français ou étrangers, des laboratoires publics ou privés.

In-situ monitoring of changes in ultrastructure and mechanical properties of flax cell walls during controlled heat treatment[☆]

Elouan Guillou^{a,b}, Loïc Dumazert^c, Célia Caër^d, Alexandre Beigbeder^a, Pierre Ouagne^e, Gwenn Le Saout^f, Johnny Beaugrand^g, Alain Bourmaud^{b,*}, Nicolas Le Moigne^{c,*}

^a IPC Laval, Rue Léonard De Vinci, Changé, France

^b Univ. Bretagne Sud, UMR CNRS 6027, IRDL, Lorient, France

^c Polymers Composites and Hybrids (PCH) – IMT Mines Ales, Ales, France

^d ENSTA Bretagne, UMR CNRS 6027, IRDL, Brest, France

^e Laboratoire Génie de Production, LGP, Université de Toulouse, INP-ENIT, Tarbes, France

^f LMGC, IMT Mines Ales, Univ Montpellier, CNRS, Ales, France

^g UR 1268 Biopolymères Interactions Assemblages, INRAE, Nantes, France

ABSTRACT

Plant fibres are increasingly used as reinforcements, especially in thermoplastic composites. Understanding the impact of temperature on the properties of these fibres is an important issue for the manufacturing of high-performance materials with minimal defects. In this work, the structural evolution and mechanical behaviour of flax fibre cell walls were dynamically monitored by temperature-controlled X-ray diffraction and nano-indentation from 25 to 230 °C; detailed biochemical analysis was also conducted on fibre samples after each heating step. With increasing temperature up to 230 °C, a decrease in the local mechanical performance of the flax cell walls, of about – 72 % for the indentation modulus and – 35 % for the hardness, was measured. This was associated with a decrease in the packing of the cellulose crystal lattice (increase in d-spacing d_{200}), as well as significant mass losses measured by thermogravimetric analysis and changes in the biochemical composition, i.e. non-cellulosic polysaccharides attributed to the middle lamellae but also to the cell walls. This work, which proposes for the first time an in-situ investigation of the dynamic temperature evolution of the flax cell wall properties, highlights the reversible behaviour of their crystalline structure (i.e. cellulose) and local mechanical properties after cooling to room temperature, even after exposure to high temperatures.

Keywords:

Flax fibre bundles

Temperature

X-ray diffraction

Nanoindentation

Biochemical analysis

Local mechanical properties

1. Introduction

Over the past decades, there has been tremendous interest and technological development concerning plant fibre reinforced composites due to their high specific mechanical properties and ecological benefits compared to synthetic fibres such as glass fibres (Lefeuvre, Bourmaud, Morvan, & Baley, 2014; Le Duigou, Davies, & Baley, 2011; Joshi, Drzal, Mohanty, & Arora, 2004; Papadopoulou et al., 2015). Environmental concerns are currently driving interest in the use of thermoplastic matrices to replace thermoset materials and pave the way for recycling and composting as end-of-life routes for plant fibre composites (Bourmaud, Shah, Beaugrand, & Dhakal, 2020; Beigbeder, Perrin, Mascaro, & Lopez-Cuesta, 2013). However, using thermoplastic polymers as a

matrix involves long processing cycles at high temperature, which may negatively affect the structure and the mechanical properties of plant fibres (Domenek et al., 2021) and their composites due to the particular composition and ultrastructure of plant fibres (Bourmaud et al., 2020; Thomason & Rudeiros-Fernández, 2021; Ramakrishnan, Le Moigne, De Almeida, Regazzi, & Corn, 2019).

Among plant fibres, flax fibres are elementary cells organized into bundles, and made up of a primary cell wall (PCW) with a thickness of around 0.2 μm and a secondary cell wall (SCW) divided into three main layers S1, S2-G and S2-Gn. The intercellular cohesion between elementary fibres is ensured by the composite middle lamella (CML). The thick cell wall S2-G, with a gelatinous appearance due to its specific composition similar to tension wood fibres, is progressively formed from

[☆] IMT Mines Ales and BIA are members of the European Polysaccharide Network of Excellence (EPNOE) <https://www.epnoe.eu>.

* Corresponding authors.

E-mail addresses: alain.bourmaud@univ-ubs.fr (A. Bourmaud), nicolas.le-moigne@mines-ales.fr (N. Le Moigne).

the conversion of the initially developed S2-Gn layer (Clair, Déjardin, Pilate, & Alméras, 2018; Gorshkova et al., 2018). The mature S2-G layer, mainly responsible for the longitudinal properties of the fibre (final thickness around 5–10 μm), is characterised by high proportion of cellulose microfibrils (between 80 and 90 % wt/%) spirally wounded at around 8° from the fibre axis (Gorshkova & Morvan, 2006; Baley et al., 2014; Melelli et al., 2021; Melelli, Jamme, Beaugrand, & Bourmaud, 2022). Besides cellulose microfibrils, the S2-G layer includes a few proteins and non-cellulosic polysaccharides (NCPs), i.e. hemicelluloses, pectins and lignin, distinguishable in two classes: (1) the structuring polysaccharides are mostly composed of hemicelluloses (mainly β -(1 \rightarrow 4)glucomannans and β -(1 \rightarrow 4)xylans) and pectic β -(1 \rightarrow 4)galactans that have a degree of polymerization (DP) higher than 10 and (2) the matrix polysaccharides containing pectins, i.e. rhamnogalacturonan I (RG-I), and homogalacturonan (HG) (Gorshkova et al., 2003; Gorshkova & Morvan, 2006; Melelli et al., 2022). A multilayer composite model was proposed by Rihouey, Paynel, Gorshkova, and Morvan (2017). As the cellulose content, and in particular, the cellulose crystallinity and microfibrillar angle (MFA) play a key role in the fibre tensile behaviour, the matrix polysaccharides are more involved in the load transfer whereas structuring polysaccharides ensure the cohesion between cellulose microfibrils and contribute to the stiffness of the fibre (Shah, 2013; Bledzki & Gassan, 1999; Bourmaud et al., 2013; Lefeuvre et al., 2015). Previous works evidenced that cellulose crystallinity (Bourmaud et al., 2013) and content (Nuez et al., 2020) are positively correlated to fibre properties or the associated composite materials.

It is also known that mechanical properties of elementary flax fibres are affected by heat treatments, especially during composite's manufacturing, primarily because of the thermal sensitivity of NCPs (Bourmaud et al., 2020). Several research works highlighted a loss of mechanical properties of natural fibres starting at temperatures above 170 °C (Gassan & Bledzki, 2001; Placet, 2009; Bourmaud, Le Duigou, Gourier, & Baley, 2016; Thomason & Rudeiros-Fernández, 2021). However, structural changes of cellulose and the impact on mechanical properties has not been studied in-situ for flax fibres during a dynamic heat treatment, which is more representative than a pre-heating treatment followed by analysis after cooling. Of the two conformations of cellulose ($I\alpha$ and $I\beta$), $I\beta$ is found in both bast fibres and tension wood. The latter is well documented, especially the impact of temperature on structural changes of cellulose. Diffraction methods stated that the d-spacings of crystallographic planes evolve with temperature, highlighting the anisotropic thermal expansion behaviour of cellulose $I\beta$ in wood (Poletto, Zattera, Forte, & Santana, 2012; Wada, Hori, Kim, & Sasaki, 2010; Hori & Wada, 2005). As far as cellulose $I\beta$ in flax fibres is concerned, no data is available to our knowledge.

In the present study, the impact of cellulose structural changes and NCPs thermal degradation from 25 to 230 °C on mechanical properties of elementary flax fibre was investigated. The evolution of local mechanical properties by nanoindentation and cellulose structure through X-ray diffraction (XRD) was monitored during dynamic heating. The originality of this work is to assess in-situ the mechanical properties and changes in ultrastructure of flax fibre during heat treatment. In addition, biochemical composition of fibre was analysed before and after thermal treatment. Deeper insights are given about the correlation between NCPs thermal degradation, ultrastructure evolution and mechanical behaviour of flax fibre.

2. Materials and methods

2.1. Flax fibres

Flax fibre bundles were extracted from a 80 g/m² Flaxtape unidirectional (UD) reinforcement kindly provided by Ecotechnil company (Yvetot, France). The UD reinforcement is an assembly of different flax batches. These textile flax varieties were grown in Normandy in 2020 and field dew-retted for 4–6 weeks depending on weather conditions.

2.2. Methods

2.2.1. Thermogravimetric analysis (TGA)

The thermal stability of flax fibres was evaluated with a TGA 8000 device (Perkin Elmer). For each experiment, 10 mg of flax fibres bundles were placed in the crucible. The changes in mass as a function of temperature were measured from 30 °C to 900 °C with a heating rate of 10 °C/min under air (40 mL/min). The degradation kinetic of flax fibres was also studied by TGA for different isothermal temperatures with 120 min isotherm steps at 170 °C, 190 °C, 210 °C and 230 °C. Finally, in order to simulate the heating cycles applied for the XRD and nanoindentation experiments, a multi-step program was used: an initial isotherm at 30 °C for 1 min for stabilisation, followed by successive heating ramps (30 °C/min under air 40 mL/min) and isotherms at pre-defined temperatures (170 °C, 190 °C, 210 °C and 230 °C) with a 20 min isotherm step at each temperature, mimicking of the heating conditions and isotherm steps used for the XRD and nanoindentation temperature-controlled experiments.

2.2.2. Temperature-controlled X-ray diffractometry (XRD)

Bruker D8 Advance diffractometer (θ - θ configuration using CuK α radiation) was used with a fixed divergence slit 0.3° and the LynxEye Position Sensitive Detector. For in-situ temperature studies, disk-shaped pressed flax fibres bundles were placed in alumina ceramic sample holder cup (18 mm diameter, 0.8 mm deep) and positioned in a high temperature chamber (HTK 1200, Anton Paar). The accuracy of the temperature measurement was previously checked by thermal expansion of periclase. The samples were then heated at a rate of 30 °C/min up to 230 °C. At 25, 170, 190, 210, 230 °C, and after cooling (25 °C), the temperature was kept constant and scans were collected in the 10–50° 2 θ range with a step size of 0.009° and an acquisition time of about 16 min. The d-spacings were calculated using the Bragg equation based on the peak position of the 200 plane.

2.2.3. Biochemical analysis

2.2.3.1. Monosaccharide composition. Identification and quantification of neutral monosaccharides were performed by gas chromatography after acid hydrolysis and conversion of monomers into alditol acetates, according to (Gautreau et al., 2022). Peak separation and identification were done thanks to a Gas Chromatography (TraceGOLD™ Thermo Scientific™) with a TG-225MS GC Column (30 \times 0.32 mm ID). For calibration, external standards (Glucose, galactose, mannose, rhamnose, xylose, arabinose), and inositol as internal standard were used. Uronic acids (glucuronic acid and galacturonic acid) in acid hydrolysates were quantified using the methoxydiphenyl colorimetric method (Blumenkrantz & Asboe-Hansen, 1973). All tests were done in triplicate independent samples.

2.2.3.2. Lignin analysis. The lignin content was quantified in homogenised powdered particles of samples. The lignin content was calculated by spectrophotometry measurement following the acetyl bromide method (Hatfield & Fukushima, 2005). The sample mass was set to approximately 20 mg per assay. All chemicals were laboratory grade from Sigma Aldrich (St. Louis, USA), and the analyses were performed with three independent analyses, the lignin content expressed as a percentage of the flax fibre bundles dry matter.

2.2.4. SEM observations

The ultrastructure of flax fibres heated at different isothermal temperatures (170, 190, 210 and 230 °C) was observed by scanning electron microscope (SEM) (Quanta FEG 200, FEI Company). The fibre samples were deposited on the sample holder with carbon tape and sputter coated with carbon using a Carbon Evaporator Device CED030 (Balzers). The acceleration voltage was set to 12.5 kV.

2.2.5. Temperature-controlled nanoindentation

2.2.5.1. Sample preparation. The flax fibre bundles were cut to lengths of <5 mm and placed in a flat silicone embedding mould (Polysciences) in the longitudinal direction. Replicate of flax fibre bundles were embedded in epoxy resin (DP760 3M™ Scotch-Weld) and placed in an oven at 50 °C overnight to cure the resin. It was indented in thickness to a final height of about 4 mm, and then glued to a 12 mm stainless steel mounting disc for nanoindentation. The sample surface was cut using an ultramicrotome (Ultracut S, Leica Microsystems SAS, France) equipped with diamond knives (Histo and Ultra AFM, Diatome, Switzerland) to obtain flat surface by trimming thin sections (final thickness of approximately 50 nm) at a reduced cutting speed (~1 mm/s) to minimise compression and sample deformation during the cutting process and thereby reduce sample surface damages and excessive topography variations.

2.2.5.2. Nanoindentation experimental protocol.

measurements were conducted using a TI 980 Triboindenter device (Bruker Hysitron), fitted with a numerical microscope and a NanoDMA III transducer. Temperature tests were performed using an xSol 400 (Bruker Hysitron) heating stage placed into the TI980 chamber. Due to the mounting, the sample is only reachable through a hole in the xSol top stage. A specific elongated probe has then to be used to indent the sample through the height of the heating stage. The probe used in this study is a Berkovich-shaped diamond tip.

Prior to nanoindentation experiments, all calibrations were successfully performed at ambient temperature (i.e. indentation axis, optic-probe tip offset, machine compliance and probe tip area function). The sample was then placed into the xSol 400 heating stage. The study is conducted on a carefully selected bundle of fibres, showing at least eight well cut and large fibre bundle, with suitable orientation, perpendicular to the cutting plane. The heating rate was fixed to 20 °C/min and stopped at several predefined temperatures: 25, 75, 125, 170, 190, 210, 230 °C, and back to 25 °C. Each isothermal step lasted approximately 20 min, except for the last one, i.e. the return to ambient temperature, which was performed 12 h after the 230 °C isothermal step. A different

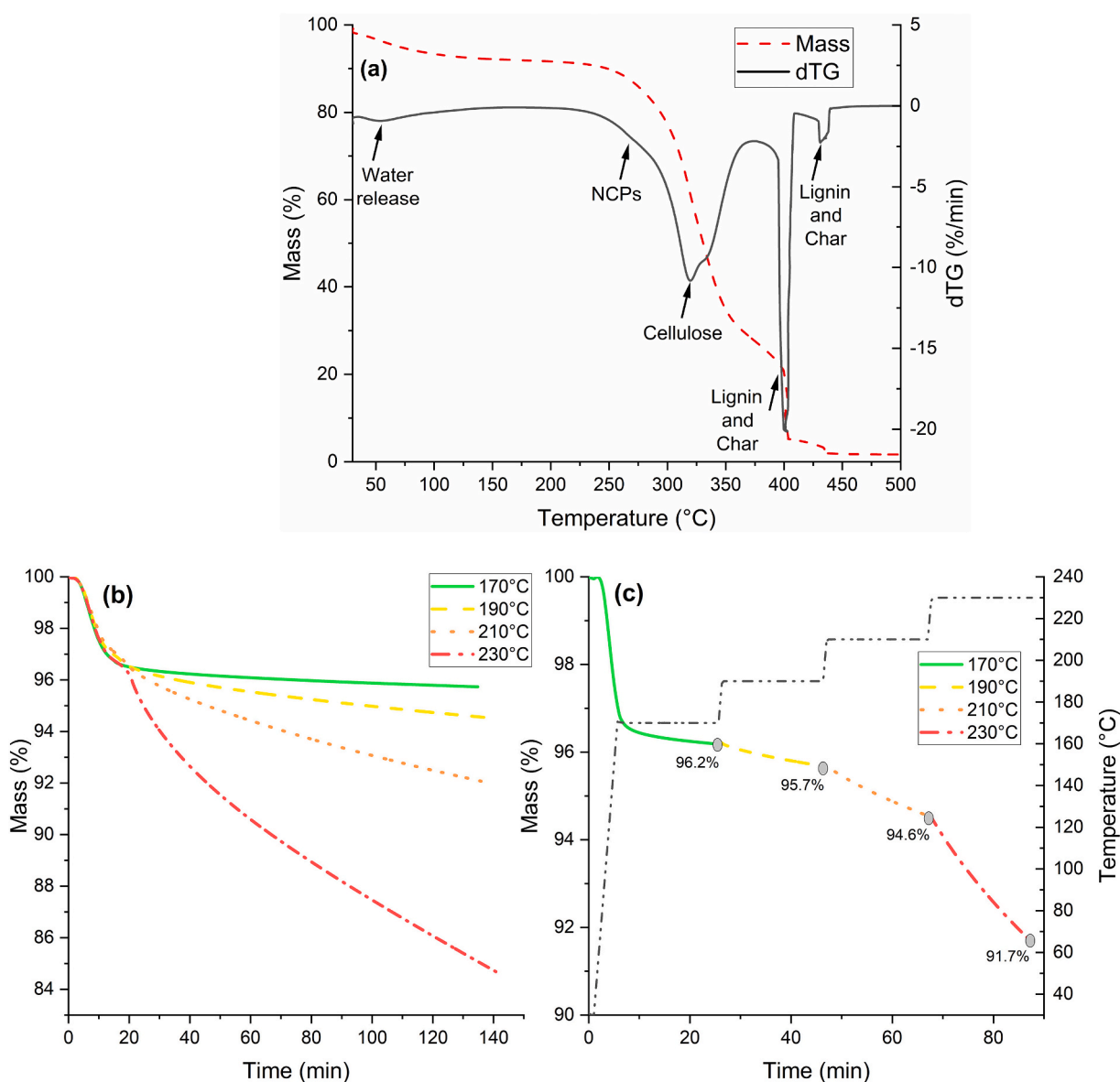


Fig. 1. (a) Mass loss and dTG curves of flax fibre bundles during heating at 10 °C/min under air, arrows indicate mass losses and degradation events; (b) Thermal degradation kinetics of flax fibres at different isothermal temperatures under air; (c) Simulated thermal degradation of flax fibres during temperature-controlled XRD and nanoindentation experiments with successive 20 min isotherms at 170 °C, 190 °C, 210 °C and 230 °C under air.

flax fibre was indented at each isothermal step, with several individual flax fibre tested.

For each isotherm, several operations were performed. First, 5–10 min were needed to reach temperature stabilisation, then surface height was detected thanks to a 2 μN indentation load in an area close but external to the chosen flax fibre. Nanoindentation tests were finally performed using an XPM very fast indentation mapping (Bruker Hysitron). The indentation mapping was centered on a flax fibre, and consisted in an array of 11×11 load-controlled indentations up to 180 μN . The space between indents was set to 2 μm . Thanks to this procedure, a mapping of mechanical properties is obtained (i.e. hardness and indentation modulus, both calculated according to [Oliver & Pharr, 1992](#)). The indentation modulus calculation takes into account elastic's modulus and Poisson's ratio of both specimen and indenter. This temperature-controlled nanoindentation protocol was applied on three different samples, so-called samples 1, 2 and 3.

3. Results and discussion

3.1. Thermal stability and degradation kinetics of flax fibres bundles

The thermal stability of flax fibres bundles was studied using TGA. The change in mass versus temperature is shown in [Fig. 1a](#). Beyond the first peak appearing at around 50–100 $^{\circ}\text{C}$ and corresponding to the release of water, three degradation steps associated to weight losses are generally observed in the derivative thermogravimetric (dTG) curves of flax fibres under air. The degradation event at $\sim 275^{\circ}\text{C}$, which can be seen in [Fig. 1a](#) as a very small shoulder on the main peak is related in the literature to the degradation of low molecular weight NCPs such as hemicelluloses (especially xylan in the case of flax bast fibre), pectins and waxes. The main peak is associated to the degradation of cellulose and occurs at 320 $^{\circ}\text{C}$ with a shoulder at 335 $^{\circ}\text{C}$ ([Shafizadeh & Lai, 1972](#); [Dorez, Ferry, Sonnier, Taguet, & Lopez-Cuesta, 2014](#); [Thomason & Rudeiros-Fernández, 2021](#)). It should be pointed out that the degradation of lignin generally occurs over a wide temperature range, i.e. from 200 to 500 $^{\circ}\text{C}$ ([Dorez et al., 2014](#); [Yu, Sun, Ma, Qiao, & Yao, 2016](#)). The third degradation event which extends from 375 to 440 $^{\circ}\text{C}$ corresponds to the thermal degradation of aromatic rings of lignin and of the char formed during the first degradation steps ([Tejado, Peña, Labidi, Echeverria, & Mondragon, 2007](#); [Bentez-Guerrero, López-Beceiro, Sánchez-Jiménez, & Pascual-Cosp, 2014](#)).

The time of exposure to high temperatures is also critical, and the thermal degradation kinetics of flax fibre bundles for different isotherms is shown in [Fig. 1b](#). Significant variations in mass loss over time can be observed and the extent of degradation increases drastically with increasing isothermal temperatures. During the first 20 min, the flax fibre bundles lost about 3.5–4 % mass upon heating, corresponding to the water release. This mass loss is followed by a slow decrease in mass reaching 4.2 % and 5.3 % after 120 min of isotherm at 170 $^{\circ}\text{C}$ and 190 $^{\circ}\text{C}$. This mass loss is more pronounced at 190 $^{\circ}\text{C}$, which should be related to the degradation of NCPs that begins to occur ([Domenek et al., 2021](#)). At 210 $^{\circ}\text{C}$ and above, water release is followed by a pronounced degradation of NCPs (and possibly cellulose) that begins to occur after 20 min of exposure. Mass losses after 120 min isotherms reach up to 7.5 % and 13.9 % at 210 $^{\circ}\text{C}$ and 230 $^{\circ}\text{C}$, respectively.

Based on these results, the thermal degradation of flax fibres was simulated based on similar heating conditions used in temperature-controlled XRD and nanoindentation experiments conducted at successive isotherms ([Fig. 1c](#)). As discussed above, it appears that water release is mainly responsible for the first mass loss (about 3.5 %) up to 170 $^{\circ}\text{C}$. Then, the degradation kinetics greatly increases with a drastic mass loss of $>8\%$ (including the water release) at the end of the 90 min multi-isothermal cycle. This confirms that a significant part of organic compounds (about 4.5 %), mainly NCPs, are degraded during the temperature-controlled XRD and nanoindentation experiments.

These analyses are also supported by the visual observations shown

in [Fig. 2a](#), where a darkening of the fibres is clearly visible above 190 $^{\circ}\text{C}$, evidencing major structural and biochemical changes after heating. SEM pictures reveal that heating the fibres up to 230 $^{\circ}\text{C}$ ([Fig. 2f](#) and [g](#)) strongly degraded the NCPs from the composite middle lamella CML (i.e. mostly amorphous polysaccharide) leading to the decohesion of the bundles and its separation into elementary fibres ([Gautreau et al., 2022](#)). One can expect that NCPs from the cell walls have been also partially degraded but this cannot be visualized by SEM. To this aim, the evolution of monosaccharide components as a function of temperature will be specifically addressed in [Section 3.3](#).

3.2. Evolution of cellulose crystalline structure by temperature-controlled XRD

The XRD pattern in [Fig. 3a](#) is characterised by a well-defined peak at around 22.9 $^{\circ}$ and two secondary peaks at 15.1 $^{\circ}$ and 16.8 $^{\circ}$ that correspond to cellulose I ([Foner & Adan, 1983](#)) and respectively indexed as 200, 1 $\bar{1}0$ and 110. A shift is clearly observable to lower angle of the 200 peak with rising temperature due to lateral expansion of cellulose I. As seen in [Fig. 3b](#), d-spacing d_{200} is increasing with temperature from 0.388 nm at 25 $^{\circ}\text{C}$ to 0.406 nm at 230 $^{\circ}\text{C}$. Previous temperature-controlled XRD experiments on wood and algal cellulose crystals showed very similar behaviour ([Hori & Wada, 2005](#)).

As shown in the lower pattern of [Fig. 3a](#), the position of the 200 peak is very close to its initial position upon returning to room temperature. This is also attested by the d-spacing d_{200} that is roughly 0.388–0.393 nm after cooling ([Fig. 3b](#)). The lateral expansion of cellulose I that occurs with increasing temperature is therefore fully reversible and the strain induced by the temperature change does not involve any irreversible plastic mechanism in crystalline cellulose. As found by [Wada et al. \(2010\)](#), cellulose I β shows an anisotropic thermal expansion in the lateral direction, with the expansion along the [100] direction, i.e. a-axis, compared to the [010] direction, i.e. b-axis, being more pronounced because weak Van der Waals forces are present along the [100] direction while strong intermolecular hydrogen bonds are present along the [010] direction. These structural features were also confirmed for cellulose I β by density functional theory (DFT) calculations ([Dri et al., 2014](#)), and could explain the reversible lateral expansion of the cellulose crystal structure observed in the 25 $^{\circ}\text{C}$ –230 $^{\circ}\text{C}$ temperature range for flax fibres. The positions of the two other peaks 1 $\bar{1}0$ and 110 ([Fig. 3a](#)) are more difficult to determine due to peaks overlap and increase of their line widths with temperature. The increase in line width reveals a decrease of the cellulose crystal size along 1 $\bar{1}0$ and 110 with temperature. As reported in literature, the variation of crystal size makes the determination of the Segal crystallinity index delicate ([Nam, French, Condon, & Concha, 2016](#)). One can note that the orientation of the flax fibres during experiment does not permit to observe the 004 peak (usually around 34 $^{\circ}$) and determine the unit cell parameters.

3.3. Evolution of the biochemical composition of flax cell walls with thermal treatment

3.3.1. Monosaccharide evolution

[Table 1](#) shows the monosaccharide content after each thermal treatment and [Fig. 4a](#) shows the relative fraction of each monosaccharide. If one compares the monosaccharide distribution with heating temperature in flax bundle composed of fibre cell walls bound by the middle lamella, differences can be seen in both the cellulose content (assuming that all the glucose is cellulosic), and in non-cellulosic monosaccharides (see flax cell wall structure and composition in [Fig. 5](#)). Flax fibre bundles have a non-cellulosic monosaccharide content that is first impacted by the heat treatment, as it clearly decreases once 190 $^{\circ}\text{C}$ is reached, as also evidenced by mass losses measured by TGA. One can hypothesise thank to SEM observations ([Fig. 2](#)) that the middle lamella is first or predominantly affected.

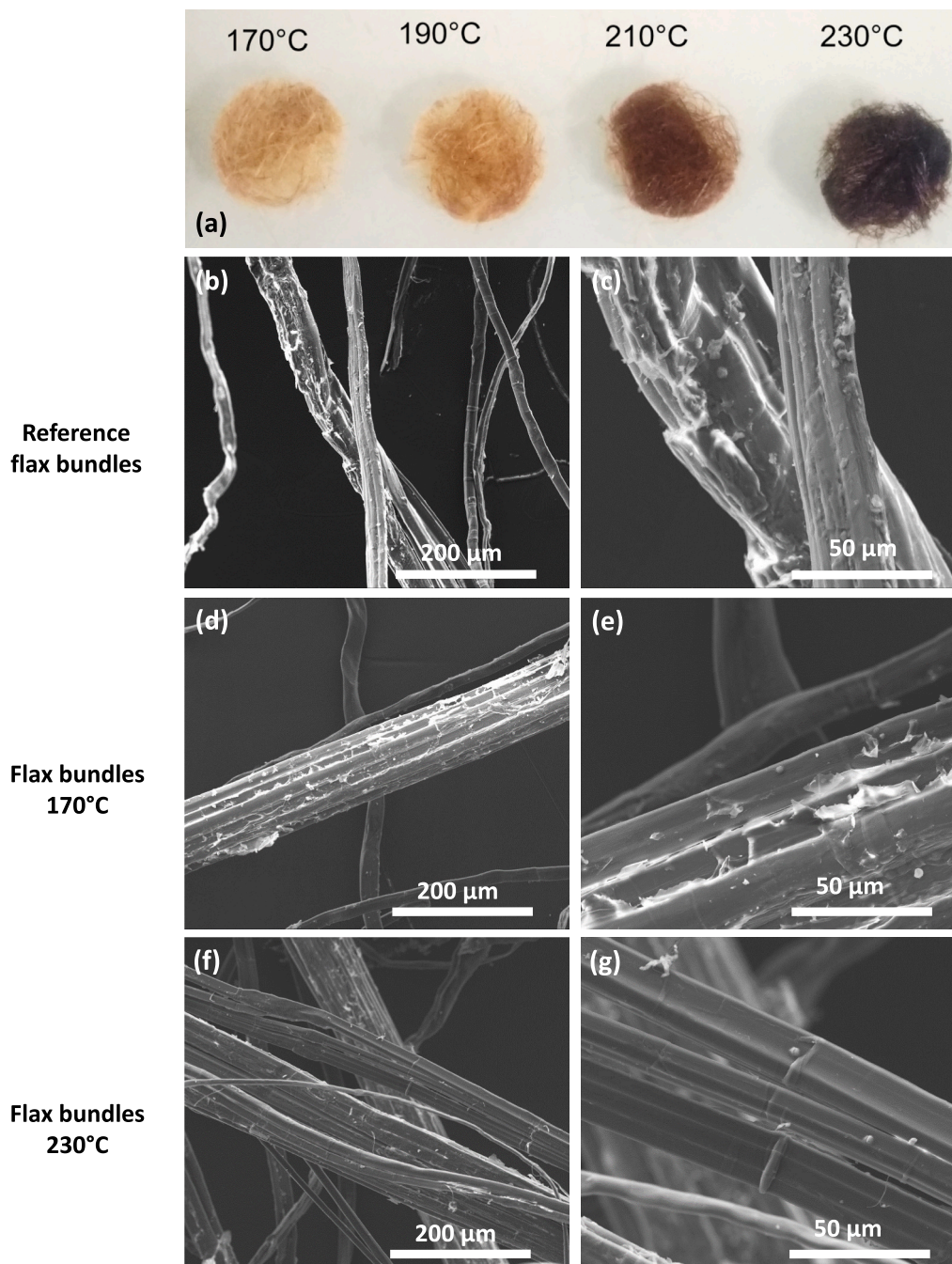


Fig. 2. (a) Visual observations of flax fibre samples at increasing temperatures and SEM observations of non-thermally treated flax bundles (b, c) and after heating at 170 °C (d, e) and 230 °C (f, g).

Those more thermosensitive polymers are often related to hemicelluloses and pectins, both ‘amorphous’ polymers. The glucose content decreases at higher temperature, i.e. above 210 °C (Fig. 4a). Glucose is the constitutive monosaccharide of cellulose but contributes also for a few to the hemicelluloses structure; we can assume that this glucose fraction attributed to NCPs is preferentially degraded above 210 °C, compared to that from cellulose.

As evidenced by the SEM observations (Fig. 2), a large part of degraded components come from regions outside the cell walls, such as CML. It has been demonstrated, on different varieties of scutched flax, that CML represents around 3 to 7.5 % in mass of dried matter (Lefeuvre, 2014; Richely, Bourmaud, Placet, Guessasma, & Beaugrand, 2022). Even if in the present work, combed fibres elements were used, SEM images show that combing is imperfect and that a significant amount of

CML is still present. CML is assumed to be mainly constituted of amorphous polymers including large amount of pectins (Homogalacturonans together with rhamnogalacturonanes type I) (Andème-Onzighi, Girault, His, Morvan, & Driouich, 2000; Jauneau, Cabin-Flaman, Verdus, Ripoll, & Thellier, 1994; Snegireva et al., 2010), xyloglucan and cellulose in low quantity (Richely et al., 2022). The main components of these pectic polymers are galacturonic acid (mostly attributed to Homogalacturonans), galactose, rhamnose (mostly attributed to rhamnogalacturonanes type I or II), arabinose, and xylose. In particular, the observed decrease in galacturonic acid, galactose, arabinose and rhamnose, poorly represented in S2-G, can be mainly attributed to CML and PCW degradation after the first heating steps. The other monosaccharides, such as mannose and xylose, are more constitutive of structural hemicelluloses present in cell walls (xylomannans and other, galactomannans

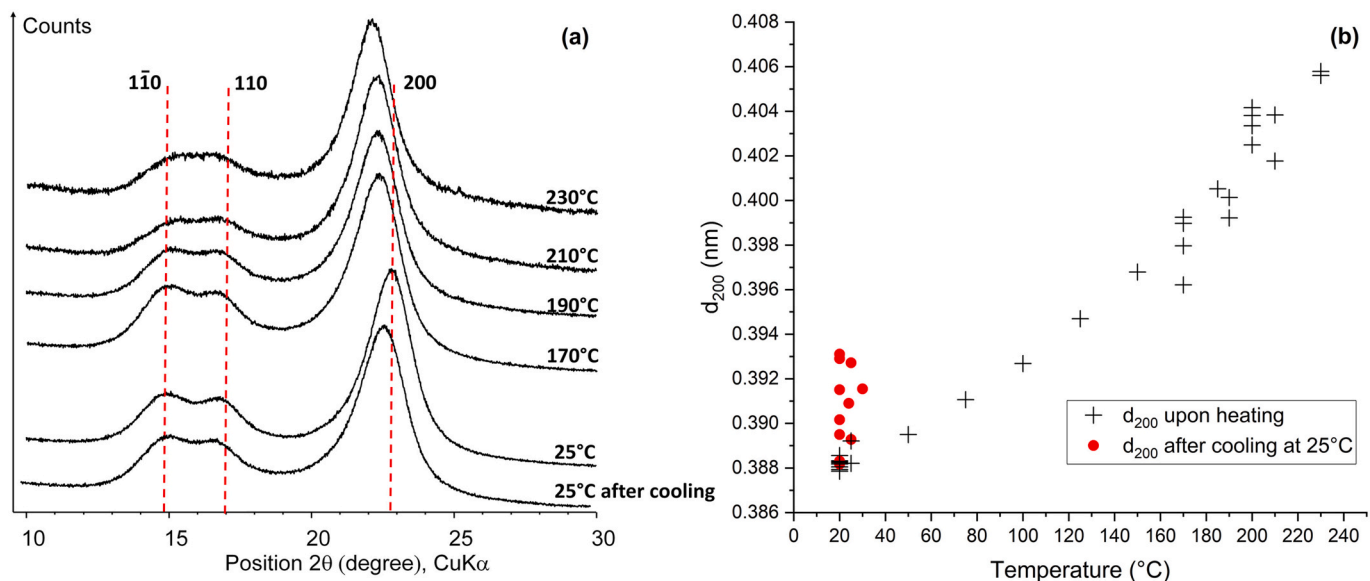


Fig. 3. (a) In-situ monitoring of diffraction patterns of flax fibres Bundles as a function of temperature by temperature-controlled XRD experiments (the lower pattern corresponds to the sample at 25 °C after cooling); (b) Variation of the d-spacing d_{200} of cellulose I in flax fibres upon heating and after cooling at 25 °C.

Table 1

Monosaccharides and lignin contents (in wt% of dry matter) for reference flax fibre bundles and after each thermal treatment, i.e. 170, 190, 210 and 230 °C.

Monosaccharides; lignin/samples	Reference flax bundles	Flax bundles 170 °C	Flax bundles 190 °C	Flax bundles 210 °C	Flax bundles 230 °C
Glucose (glc)	74.1 ± 0.7	75.3 ± 0.0	74.2 ± 0.9	72.8 ± 0.1	69.9 ± 1.1
Galactose (gal)	4.0 ± 0.1	4.1 ± 0.2	3.8 ± 0.0	2.3 ± 0.0	1.1 ± 0.2
Mannose (man)	3.6 ± 0.1	3.6 ± 0.1	3.2 ± 0.1	2.4 ± 0.1	1.5 ± 0.2
Galacturonic acid (galA)	1.9 ± 0.1	1.3 ± 0.1	0.3 ± 0.1	0.0 ± 0.0	0.0 ± 0.0
Glucuronic acid (glcA)	0.5 ± 0.1	0.6 ± 0.1	0.6 ± 0.1	0.4 ± 0.1	0.2 ± 0.1
Xylose (xyl)	1.3 ± 0.0	1.2 ± 0.1	1.2 ± 0.0	0.9 ± 0.1	0.6 ± 0.2
Arabinose (ara)	1.3 ± 0.0	1.3 ± 0.1	1.3 ± 0.1	0.8 ± 0.1	0.9 ± 0.1
Rhamnose (rha)	0.6 ± 0.1	0.7 ± 0.0	0.6 ± 0.0	0.4 ± 0.1	0.4 ± 0.1
Total monosaccharides	87.3 ± 0.5	88.2 ± 0.3	85.2 ± 0.7	80.1 ± 0.2	74.6 ± 1.0
Lignin	2.1 ± 0.1	3.0 ± 0.1	2.7 ± 0.3	3.8 ± 0.0	4.0 ± 0.2

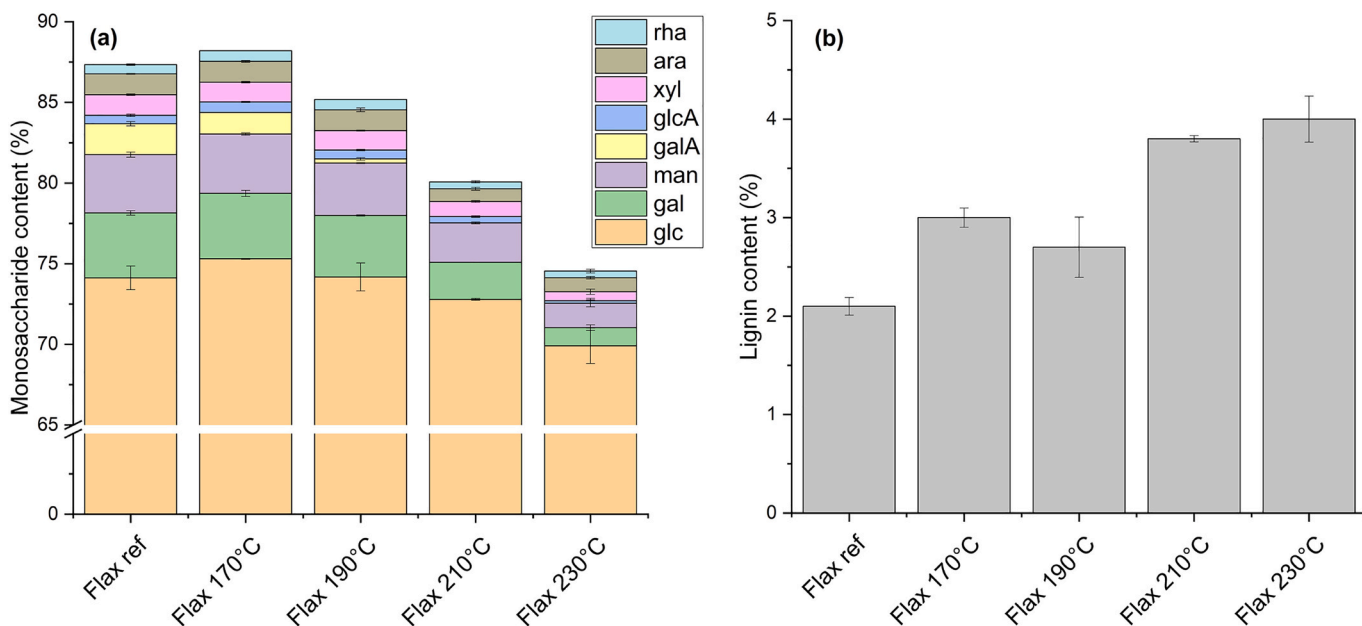


Fig. 4. (a) Monosaccharide distribution in flax fibres bundles after the different heating steps, expressed in wt% of the dry matter mass. Y-axis is truncated for better visualisation. (b) Lignin content in flax fibre bundles after the different heating steps, expressed in wt% of dry matter mass.

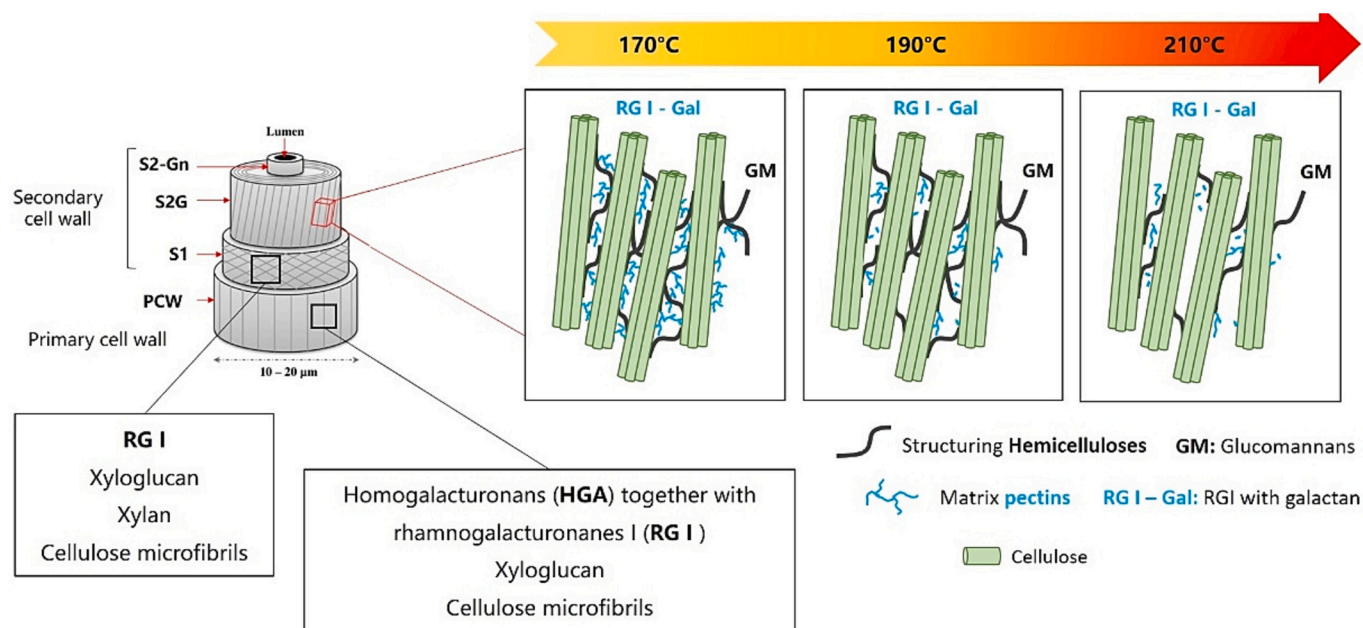


Fig. 5. Flax cell wall structure and composition and its changes upon thermal degradation focused on S2-G layer.

or glucomannans); consequently, their loss is preferentially attributed to the degradation of the S2-G layer (Fig. 5).

For all monosaccharide components, a clear decrease is demonstrated above 190 °C. This observation gives information about the thermal stability of biochemical components. Some of them are very thermo-sensitive, for example, GalA (pectins) are strongly degraded from 170 °C, while most NCPs exhibit relative stability until 190 °C. Mannose and Galactose also strongly decreases, and especially in S2-G layer from 190 °C (Fig. 4a). This is particularly important as those sugars are mostly attributed to hemicelluloses like galactomannan chains, that are reported to be responsible for the orientation and cohesion of cellulose microfibrils (Gorshkova & Morvan, 2006; Melelli et al., 2022), and consequently, their decrease may have a significant impact on cell wall mechanical properties.

3.3.2. Lignin evolution

Lignin contents are reported in Table 1. According to Fig. 4b, heating up to 230 °C leads to a gradual increase in the lignin content of the samples remaining after heating. At least a part of the lignin, the so-called condensed lignin, is reported to be thermostable. This enrichment in lignin, expressed in dry matter content, appears to be already effective at 170 °C. The 210 °C treatment has a strong impact on the polysaccharide components of the fibre since the enrichment in lignin takes a leap forward. Indeed, heated flax bundles display a huge increase by 30–50 % of the initial lignin content (set to 100 % for the non-heated reference sample). After a 230 °C heat treatment, the enrichment in lignin represent about 100 % of the initial content but the amount of lignin is still rather low (about 4 % of the dry mass). The exact nature of lignin should be further explored, before and after heat treatment, in order to unveil the fine linkages and condensation level of the lignin (Beaugrand et al., 2004).

3.4. Evolution of mechanical properties of flax cell walls by temperature-controlled nanoindentation

Fig. 6 shows an overall representation of temperature-controlled nanoindentation investigations (e.g. on Sample 2) carried out on a flax fibre bundle. Each cartography represents the indentation modulus mapping for a specific temperature. Fibres and embedding resin are quite easy to distinguish due to the high indentation modulus of flax

fibres (15–23 GPa) compared to the low indentation modulus value of resin (5–6 GPa).

In addition, Fig. 7 shows the statistical evolution of indentation modulus and hardness as a function of temperature for the three analysed samples. Each box plot represents a statistical representation of ~35 nanoindentation measurements, visually selected among the 121 indentation points performed for each temperature condition for being located in the lumen and interfacial regions were not considered. Measurements at 230 °C were not performed on Sample 1 due to issues in displacement stabilisation.

Different trends and behaviour can be highlighted for both indentation modulus and hardness evolution (Fig. 7). Indentation modulus remains stable until approximately 125 °C and then significantly decreases (p-values of 0.135 at 75 °C and 0.013 at 125 °C, based on comparison with initial values at 25 °C by the non-parametric Mann & Whitney U statistical test). Initial values are ranged between 15.5 and 23 GPa (10 %~90 %) which is well correlated with the literature (Bourmaud et al., 2016; Arnould, Siniscalco, Bourmaud, Le Duigou, & Baley, 2017). The differences in the indentation modulus between the samples could be induced by cell wall maturity, fibre orientation or MFA. Konnerth, Gierlinger, Keckes, and Gindl (2009) and Jäger, Hofstetter, Buksnowitz, Gindl-Altmutter, and Konnerth (2011) have demonstrated that increasing the MFA of cellulose induces a drop of the indentation modulus. Therefore, by analogy with the microfibril angle, even a slight misorientation of fibre should lead to data scattering. Median indentation modulus values drop to 14.2 GPa at 210 °C and 11.4 GPa at 230 °C. Considering samples 2 and 3, the decrease in the median indentation modulus between 170 °C and 230 °C reaches respectively –31 % and –33 % of its initial value. A moderate decrease in indentation modulus after heating has already been observed by Siniscalco, Arnould, Bourmaud, Le Duigou, and Baley (2018a, 2018b), with slightly different experimental protocol: the authors operated on a different fibre batch, with indentation heating time (8 min), and nanoindentation measurements were performed at room temperature, after the heat treatment. According to Siniscalco et al. (2018b), the drop of indentation modulus was attributed to a degradation of flax cell walls NCPs, i.e. pectins and hemicelluloses components, more thermo-sensitive than cellulose. In the present study, biochemical trends (see Section 3.3) show that NCPs components, which ensure stiffness due to their cohesive and structuring functions, are degraded under heating. This is in

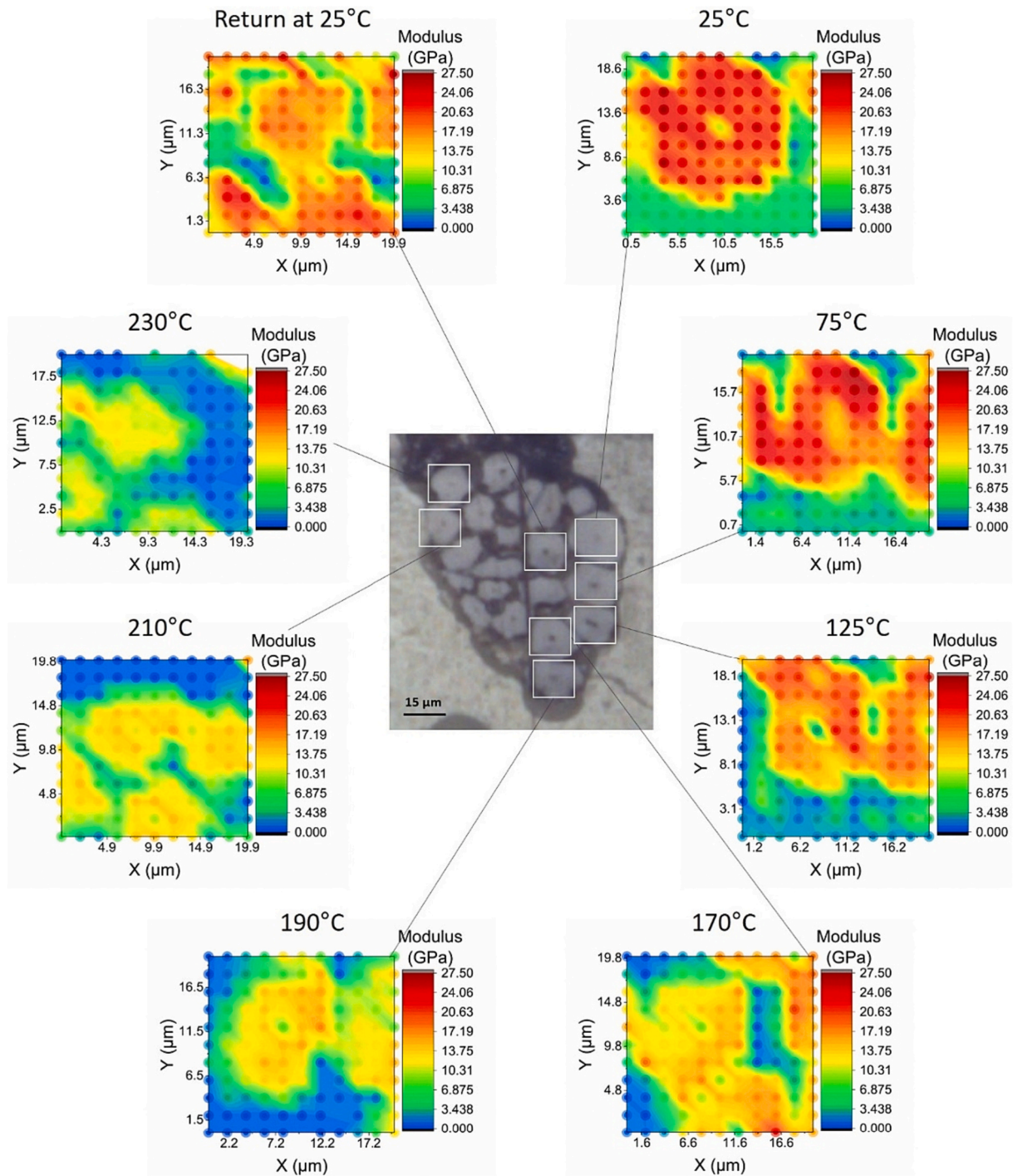


Fig. 6. In-situ monitoring of the indentation modulus by temperature-controlled nanoindentation investigations, carried out on a flax fibre bundle (e.g. on Sample 2) seen in the middle of the figure. Each cartography represents the indentation modulus x-y mapping (11×11 , i.e. 121 indentation points for each area) for a given temperature.

good agreement with the indentation modulus drop observed while increasing the temperature. Indeed, the indentation modulus obtained by indentation is not only determined by fibre longitudinal modulus but also depends on transverse and shear moduli (Eder, Arnould, Dunlop, Hornatowska, & Salmén, 2013). These moduli are very sensitive to the cell wall cohesion and may be greatly affected either by an evolution of NCPs structure or of the MFA, as assumed by Zickler, Schöberl, and Paris (2006) on pyrolysed wood cell walls. A selective degradation of NCPs and cellulose was also demonstrated on wood cell walls by Zollfrank and Fromm (2009), between 200 and 250 °C for the NCPs and after 250 °C

for cellulose. It is also well known that plant cell wall properties are strongly dependent on moisture conditions (Yu, Fei, Wang, & Tian, 2011) but the influence of humidity on nanoindentation, especially at high temperature, were not under the scope of this study.

Once the sample temperature is cooled back to 25 °C, after a long heating period at multiple isotherms (between 2 and 3 h), the indentation modulus increases (Fig. 7a and b), until approximately reaching its initial value at 25 °C (p-value of 0.007). This result indicates a reversible behaviour, which can be applied to the evolution of the indentation modulus as a function of temperature, never shown on flax cell walls, to

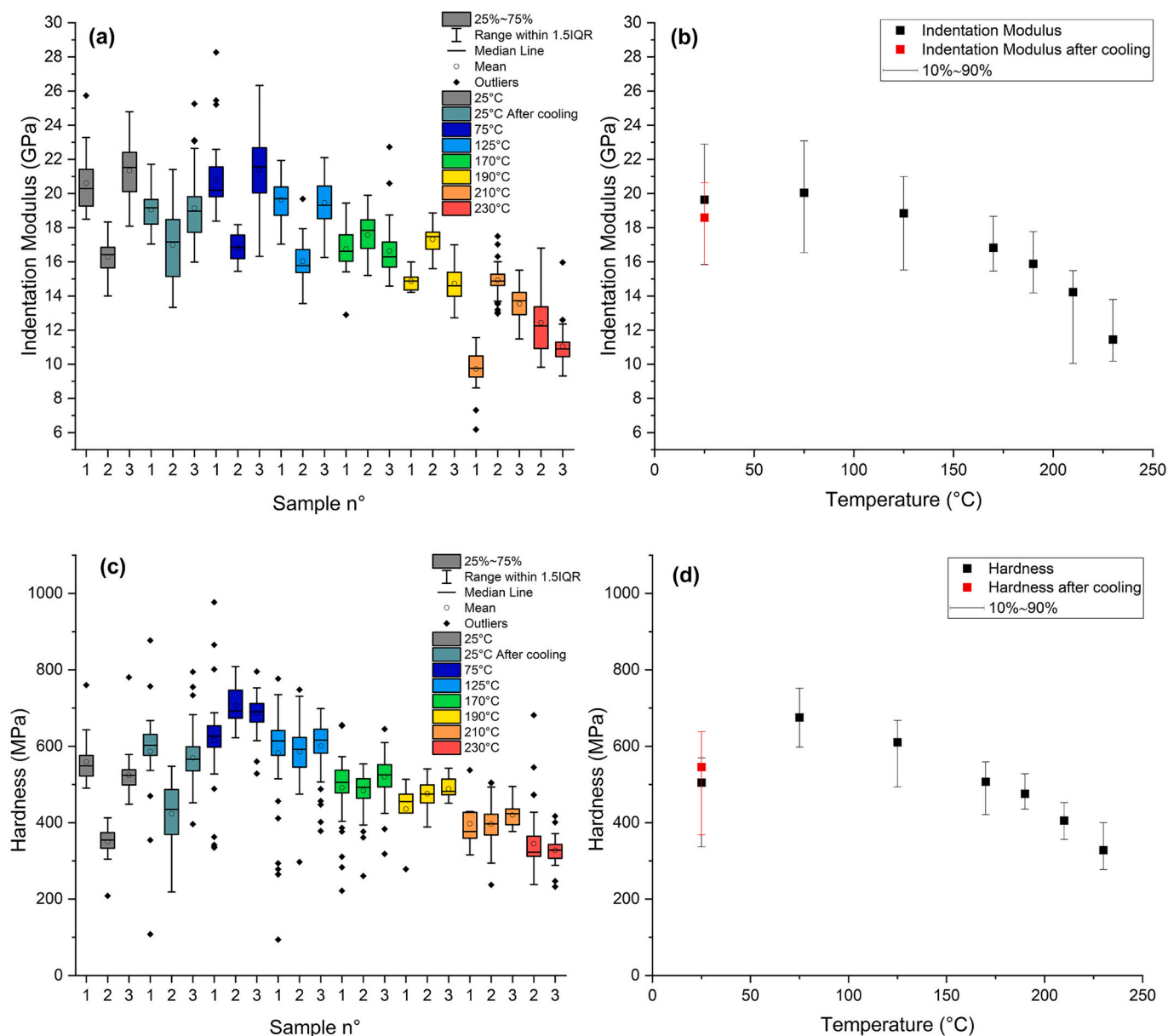


Fig. 7. Evolution of indentation modulus (a, b) and hardness (c, d) according to the temperature for the three different samples.

the best of the author's knowledge. XRD experiments (see Section 3.2) revealed an increase in d-spacing d_{200} indicating a lower compaction degree of the cell wall at high temperature, with potential consequences in terms of local stiffness. After cooling down the sample to room temperature, initial d-spacing d_{200} values were recovered, attesting for a reversible phenomenon similar to the evolution of the indentation modulus with temperature. Both temperature-controlled XRD and nanoindentation experiments confirm the major role of cellulose in stiffness values, as well as its reversible structural and mechanical behaviour with temperature, even when high temperature (i.e. 230 °C) are reached.

With regard to hardness, the trends in hardness values as a function of temperature for the three samples analysed are highly reproducible (Fig. 7c). This supports the interest of monitoring the hardness. Unlike stiffness, there is no clear trend between hardness and MFA, but hardness is also a relevant indicator of cell wall mechanical behaviour, generally more significantly affected by NCPs changes than the indentation modulus (Eder et al., 2013). This has been demonstrated on wood cell walls having different lignin content (Gindl, Gupta, & Grünwald,

2002), maturity degree (Stanzl-Tschegg, Beikircher, & Loidl, 2009) or even after thermal treatment (Yin, Berglund, & Salmén, 2011). Here, hardness values at room temperature are included between 350 and 550 MPa (10 %–90 %). It is in good agreement with literature (Bourmaud, Åkesson, et al., 2016). For the three samples, an increase in hardness (Fig. 7d) is noticed from 25 °C to 75 °C (p-value $\ll 0.001$), probably induced by the partial release of water in the flax cell walls that is likely to modify the mechanical behaviour of NCPs. At temperatures above 75 °C, constant and regular decrease of hardness is observed with a final median hardness value of 328 MPa at 230 °C. This behaviour suggests some significant changes in NCPs components, driven by their temperature sensitivity and their low glass temperature, generally assumed about 50 °C. As already observed for indentation modulus, once the sample temperature is back to ambient, the hardness increases again (Fig. 7d), showing values similar to the initial ones (but with low p-value $\ll 0.001$). This recovery of mechanical properties observed upon return to room temperature for both modulus and hardness may be due to opposite effects, i.e. the loss of modulus and hardness due to cell wall degradation, in particular NCPs, upon heating is counterbalanced by

water release and cellulose and lignin enrichment which contribute to increase the elastic mechanical properties.

It should also be noted that these nanoindentation results were obtained at the cell wall scale and not the fibre scale, which suggests a scaling factor in the study of the mechanical behaviour of flax fibres. Indeed, previous studies at the fibre scale (Gourier, Le Duigou, Bourmaud, & Baley, 2014; Siniscalco et al., 2018b) performed on different batches of single flax fibres have shown a clear drop and no recovery of tensile performances after heating, suggesting that performance at break is more impacted than performance in the elastic domain. It is thus relevant to study both scales to better understand the mechanical behaviour of flax fibres that is also dependent on other parameters such as kink-bands sensitivity, especially after heat treatment, or other layers (PCW, S1, S3-Gn) which are made of different constituents.

4. Conclusions

The evolution of the ultrastructure and local mechanical properties of flax cell walls was monitored during dynamic heating from 25 °C to 230 °C by temperature-controlled X-ray diffraction and nanoindentation experiments. This work on flax fibre bundles has highlighted for the first time, the reversible behaviour of the crystalline structure (i.e. cellulose) and mechanical properties of flax cell walls after cooling to room temperature, even after exposure to high temperature (i.e. 230 °C). Most NCPs showed relative thermal stability up to 190 °C but significant mass losses and changes in the biochemical composition of the middle lamellae and flax cell walls were observed and correlated with a decrease in local mechanical properties above 170 °C, i.e. about -72 % for indentation modulus and -35 % for hardness measured at 230 °C. The recovery of mechanical property upon return to room temperature is discussed considering offsetting effects and scaling factor. The degradation of NCP components upon heating is assumed to be responsible for a decrease in the local mechanical performance of flax cell walls, but this is counterbalanced by a decrease in cell wall moisture content and a relative enrichment in cellulose and lignin, which has a positive impact on cell wall stiffness and hardness measured by nanoindentation. These results and assumptions open scientific perspectives to go further on the understanding of microstructural and mechanical behaviour of flax cell walls when exposed to temperature. More in-depth investigations of the local mechanical behaviour of the cell walls could be conducted, in particular by analysing their visco-elasto-plastic behaviour and the relaxation contribution of the biopolymers that build up the cell walls. Moreover, a fine study by solid-state NMR and high-resolution X-ray tomography of the microstructure and micro/nano porosity, which are likely to be modified by the degradation of NCPs, would certainly improve the interpretation of the results.

CRedit authorship contribution statement

Elouan Guillou: Experimental, Methodology, Investigation, Resources, Writing - Original Draft - Review & Editing

Loïc Dumazert: Experimental (Thermogravimetric analysis), Writing - Review & Editing

Célia Caër: Experimental (nanoindentation measurements), Methodology, Investigation, Writing - Review & Editing

Alexandre Beigbeder: Writing - Review & Editing

Pierre Ouagne: Writing - Review & Editing

Gwenn Le Saout: Experimental (XRD measurements), Methodology, Validation, Resources, Writing - Review & Editing

Johnny Beaugrand: Conceptualization, Experimental, Methodology, Validation, Resources, Writing - Review & Editing, Supervision, Project administration

Alain Bourmaud: Conceptualization, Experimental, Methodology, Validation, Resources, Writing - Review & Editing, Supervision, Project administration

Nicolas Le Moigne: Conceptualization, Experimental, Methodology,

Validation, Resources, Writing - Review & Editing, Supervision, Project administration

Declaration of competing interest

The authors declare that they have no known competing financial interests or personal relationships that could have appeared to influence the work reported in this paper.

Data availability

Data will be made available on request.

Acknowledgements

The authors would like to gratefully acknowledge Laval Agglomération (<https://www.agglo-laval.fr>) and the Région Pays de Loire (<https://www.paysdelaloire.fr/>) for funding the PhD thesis of Elouan Guillou. Also, the authors wish to acknowledge Dr. Delphin Pantaloni for his experimental contribution to this work.

References

- Andème-Onzighi, C., Girault, R., His, I., Morvan, C., & Driouch, A. (2000). Immunocytochemical characterization of early-developing flax fiber cell walls. *Protoplasma*, 213(3–4), 235–245. <https://doi.org/10.1007/BF01282161>
- Arnould, O., Siniscalco, D., Bourmaud, A., Le Duigou, A., & Baley, C. (2017). Better insight into the nano-mechanical properties of flax fibre cell walls. *Industrial Crops and Products*, 97, 224–228. <https://doi.org/10.1016/j.indcrop.2016.12.020>
- Baley, C., Le Duigou, A., Bourmaud, A., Davies, P., Nardin, M., Morvan, C., ... Morvan, C. (2014). Strategy of bio-based resources: Material versus energy and Klanarong Sriroth. In *Bio-based composites for high-performance materials* (pp. 36–55). <https://doi.org/10.1201/b17601-7>
- Beaugrand, J., Crônier, D., Thiebeau, P., Schreiber, L., Debeire, P., & Chabbert, B. (2004). Structure, chemical composition, and xylanase degradation of external layers isolated from developing wheat grain. *Journal of Agricultural and Food Chemistry*, 52(23), 7108–7117. <https://doi.org/10.1021/jf049529w>
- Beigbeder, J., Perrin, D., Mascaro, J.-F., & Lopez-Cuesta, J.-M. (2013). Study of the physico-chemical properties of recycled polymers from waste electrical and electronic equipment (WEEE) sorted by high resolution near infrared devices. *Resources, Conservation and Recycling*, 78, 105–114. <https://doi.org/10.1016/j.resconrec.2013.07.006>
- Benítez-Guerrero, M., López-Beceiro, J., Sánchez-Jiménez, P. E., & Pascual-Cosp, J. (2014). Comparison of thermal behavior of natural and hot-washed sisal fibers based on their main components: Cellulose, xylan and lignin. TG-FTIR analysis of volatile products. *Thermochimica Acta*, 581, 70–86. <https://doi.org/10.1016/j.tca.2014.02.013>
- Bledzki, A., & Gassan, J. (1999). Composites reinforced with cellulose based fibres. *Progress in Polymer Science*, 24(2), 221–274. [https://doi.org/10.1016/S0079-6700\(98\)00018-5](https://doi.org/10.1016/S0079-6700(98)00018-5)
- Blumenkrantz, N., & Asboe-Hansen, G. (1973). New method for quantitative determination of uronic acids. *Analytical Biochemistry*, 54(2), 484–489. [https://doi.org/10.1016/0003-2697\(73\)90377-1](https://doi.org/10.1016/0003-2697(73)90377-1)
- Bourmaud, A., Åkesson, D., Beaugrand, J., Le Duigou, A., Skrifvars, M., & Baley, C. (2016). Recycling of L-poly-(lactide)-poly-(butylene-succinate)-flax biocomposite. *Polymer Degradation and Stability*, 128, 77–88. <https://doi.org/10.1016/j.polymerdegradstab.2016.03.018>
- Bourmaud, A., Le Duigou, A., Gourier, C., & Baley, C. (2016). Influence of processing temperature on mechanical performance of unidirectional polyamide 11-flax fibre composites. *Industrial Crops and Products*, 84, 151–165. <https://doi.org/10.1016/j.indcrop.2016.02.007>
- Bourmaud, A., Morvan, C., Bouali, A., Placet, V., Perré, P., & Baley, C. (2013). Relationships between micro-fibrillar angle, mechanical properties and biochemical composition of flax fibers. *Industrial Crops and Products*, 44, 343–351. <https://doi.org/10.1016/j.indcrop.2012.11.031>
- Bourmaud, A., Shah, D. U., Beaugrand, J., & Dhakal, H. N. (2020). Property changes in plant fibres during the processing of bio-based composites. *Industrial Crops and Products*, 154, Article 112705. <https://doi.org/10.1016/j.indcrop.2020.112705>
- Clair, B., Déjardin, A., Pilate, G., & Alméras, T. (2018). Is the G-layer a tertiary cell wall? *Frontiers in Plant Science*, 9, 8–11. <https://doi.org/10.3389/fpls.2018.00623>
- Domenek, S., Berzin, F., Ducruet, V., Plessis, C., Dhakal, H., Richaud, E., & Beaugrand, J. (2021). Extrusion and injection moulding induced degradation of date palm fibre - polypropylene composites. *Polymer Degradation and Stability*, 190, Article 109641. <https://doi.org/10.1016/j.polymerdegradstab.2021.109641>
- Dorez, G., Ferry, L., Sonnier, R., Taguet, A., & Lopez-Cuesta, J. M. (2014). Effect of cellulose, hemicellulose and lignin contents on pyrolysis and combustion of natural fibers. *Journal of Analytical and Applied Pyrolysis*, 107, 323–331. <https://doi.org/10.1016/j.jaap.2014.03.017>

- Dri, F. L., Shang, S., Hector, L. G., Saxe, P., Liu, Z.-K., Moon, R. J., & Zavattieri, P. D. (2014). Anisotropy and temperature dependence of structural, thermodynamic, and elastic properties of crystalline cellulose I β : A first-principles investigation. *Modelling and Simulation in Materials Science and Engineering*, 22(8), Article 085012. <https://doi.org/10.1088/0965-0393/22/8/085012>
- Eder, M., Arnold, O., Dunlop, J. W. C., Hornatowska, J., & Salmén, L. (2013). Experimental micromechanical characterisation of wood cell walls. *Wood Science and Technology*, 47(1), 163–182. <https://doi.org/10.1007/s00226-012-0515-6>
- Foner, H. A., & Adan, N. (1983). The characterization of papers by X-ray diffraction (XRD): Measurement of cellulose crystallinity and determination of mineral composition. *Journal of the Forensic Science Society*, 23(4), 313–321. [https://doi.org/10.1016/S0015-7368\(83\)72269-3](https://doi.org/10.1016/S0015-7368(83)72269-3)
- Gassan, J., & Bledzki, A. K. (2001). Thermal degradation of flax and jute fibers. *Journal of Applied Polymer Science*, 82(6), 1417–1422. <https://doi.org/10.1002/app.1979>
- Gautreau, M., Durand, S., Patrel, A., Le Gall, S., Foucat, L., Falourd, X., ... Beaugrand, J. (2022). Impact of cell wall non-cellulosic and cellulosic polymers on the mechanical properties of flax fibre bundles. *Carbohydrate Polymers*, 291, Article 119599. <https://doi.org/10.1016/j.carbpol.2022.119599>
- Gindl, W., Gupta, H. S., & Grünwald, C. (2002). Lignification of spruce tracheid secondary cell walls related to longitudinal hardness and modulus of elasticity using nano-indentation. *Canadian Journal of Botany*, 80(10), 1029–1033. <https://doi.org/10.1139/b02-091>
- Gorshkova, T., Milkshina, P., Petrova, A., Chernova, T., Mokshina, N., & Gorshkov, O. (2018). Plants at bodybuilding: development of plant “Muscles.”. In *Plant biomechanics* (pp. 141–163). https://doi.org/10.1007/978-3-319-79099-2_7
- Gorshkova, T., & Morvan, C. (2006). Secondary cell-wall assembly in flax phloem fibres: Role of galactans. *Planta*, 223(2), 149–158. <https://doi.org/10.1007/s00425-005-0118-7>
- Gorshkova, T. A., Sal'nikov, V. V., Chemiksova, S. B., Ageeva, M. V., Pavlencheva, N. V., & van Dam, J. E. G. (2003). The snap point: A transition point in Linum usitatissimum bast fiber development. *Industrial Crops and Products*, 18(3), 213–221. [https://doi.org/10.1016/S0926-6690\(03\)00043-8](https://doi.org/10.1016/S0926-6690(03)00043-8)
- Gourier, C., Le Duigou, A., Bourmaud, A., & Baley, C. (2014). Mechanical analysis of elementary flax fibre tensile properties after different thermal cycles. *Composites Part A: Applied Science and Manufacturing*, 64, 159–166. <https://doi.org/10.1016/j.compositesa.2014.05.006>
- Hatfield, R., & Fukushima, R. S. (2005). Can lignin be accurately measured? *Crop Science*, 45(3), 832–839. <https://doi.org/10.2135/cropsci2004.0238>
- Hori, R., & Wada, M. (2005). The thermal expansion of wood cellulose crystals. *Cellulose*, 12(5), 479–484. <https://doi.org/10.1007/s10570-005-5967-5>
- Jäger, A., Hofstetter, K., Buksnowitz, C., Gindl-Altmatter, W., & Konnerth, J. (2011). Identification of stiffness tensor components of wood cell walls by means of nanoindentation. *Composites Part A: Applied Science and Manufacturing*, 42(12), 2101–2109. <https://doi.org/10.1016/j.compositesa.2011.09.020>
- Jauneau, A., Cabin-Flaman, A., Verdus, M.-C., Ripoll, C., & Thellier, M. (1994). Involvement of calcium in the inhibition of endopolygalacturonase activity in epidermis cell wall of Linum usitatissimum. *Plant Physiology and Biochemistry*, 32(6), 839–846.
- Joshi, S. V., Drzal, L. T., Mohanty, A. K., & Arora, S. (2004). Are natural fiber composites environmentally superior to glass fiber reinforced composites? *Composites Part A: Applied Science and Manufacturing*, 35(3), 371–376. <https://doi.org/10.1016/j.compositesa.2003.09.016>
- Konnerth, J., Gierlinger, N., Keckes, J., & Gindl, W. (2009). Actual versus apparent within cell wall variability of nanoindentation results from wood cell walls related to cellulose microfibril angle. *Journal of Materials Science*, 44(16), 4399–4406. <https://doi.org/10.1007/s10853-009-3665-7>
- Le Duigou, A., Davies, P., & Baley, C. (2011). Environmental impact analysis of the production of flax fibres to be used as composite material reinforcement. *Journal of Biobased Materials and Bioenergy*, 5(1), 153–165. <https://doi.org/10.1166/jbmb.2011.1116>
- Lefevre, A. (2014). *Contribution à l'étude des propriétés des fibres de lin (Linum usitatissimum L., variétés Marylin et Andréa) en fonction des pratiques culturales sur le plateau du Neubourg. Fibres destinées au renforcement de matériaux composites* (Doctoral dissertation, Rouen).
- Lefevre, A., Bourmaud, A., Morvan, C., & Baley, C. (2014). Tensile properties of elementary fibres of flax and glass: Analysis of reproducibility and scattering. *Materials Letters*, 130, 289–291. <https://doi.org/10.1016/j.matlet.2014.05.115>
- Lefevre, A., Le Duigou, A., Bourmaud, A., Kervoelen, A., Morvan, C., & Baley, C. (2015). Analysis of the role of the main constitutive polysaccharides in the flax fibre mechanical behaviour. *Industrial Crops and Products*, 76, 1039–1048. <https://doi.org/10.1016/j.indcrop.2015.07.062>
- Melilli, A., Durand, S., Arnould, O., Richely, E., Guessasma, S., Jamme, F., ... Bourmaud, A. (2021). Extensive investigation of the ultrastructure of kink-bands in flax fibres. *Industrial Crops and Products*, 164(August 2020), Article 113368. <https://doi.org/10.1016/j.indcrop.2021.113368>
- Melilli, A., Jamme, F., Beaugrand, J., & Bourmaud, A. (2022). Evolution of the ultrastructure and polysaccharide composition of flax fibres over time: When history meets science. *Carbohydrate Polymers*, 291, Article 119584. <https://doi.org/10.1016/j.carbpol.2022.119584>
- Nam, S., French, A. D., Condon, B. D., & Concha, M. (2016). Segal crystallinity index revisited by the simulation of X-ray diffraction patterns of cotton cellulose I β and cellulose II. *Carbohydrate Polymers*, 135, 1–9. <https://doi.org/10.1016/j.carbpol.2015.08.035>
- Nuez, L., Gautreau, M., Mayer-Laigle, C., D'Arras, P., Guillon, F., Bourmaud, A., ... Beaugrand, J. (2020). Determinant morphological features of flax plant products and their contribution in injection moulded composite reinforcement. *Composites Part C: Open Access*, 3, Article 100054. <https://doi.org/10.1016/j.jcomc.2020.100054>
- Oliver, W. C., & Pharr, G. M. (1992). An improved technique for determining hardness and elastic modulus using load and displacement sensing indentation experiments. *Journal of Materials Research*, 7(6), 1564–1583. <https://doi.org/10.1557/JMR.1992.1564>
- Papadopoulou, E., Bikiaris, D., Chrysafis, K., Wladyka-Przybylak, M., Wesolek, D., Mankowski, J., ... Gronberg, V. (2015). Value-added industrial products from bast fiber crops. *Industrial Crops and Products*, 68, 116–125. <https://doi.org/10.1016/j.indcrop.2014.10.028>
- Placet, V. (2009). Characterization of the thermo-mechanical behaviour of Hemp fibres intended for the manufacturing of high performance composites. *Composites Part A: Applied Science and Manufacturing*, 40(8), 1111–1118. <https://doi.org/10.1016/j.compositesa.2009.04.031>
- Poletto, M., Zattera, A. J., Forte, M. M. C., & Santana, R. M. C. (2012). Thermal decomposition of wood: Influence of wood components and cellulose crystallite size. *Bioresource Technology*, 109, 148–153. <https://doi.org/10.1016/j.biortech.2011.11.122>
- Ramakrishnan, K. R., Le Moigne, N., De Almeida, O., Regazzi, A., & Corn, S. (2019). Optimized manufacturing of thermoplastic biocomposites by fast induction-heated compression moulding: Influence of processing parameters on microstructure development and mechanical behaviour. *Composites Part A: Applied Science and Manufacturing*, 124, Article 105493. <https://doi.org/10.1016/j.compositesa.2019.105493>
- Richely, E., Bourmaud, A., Placet, V., Guessasma, S., & Beaugrand, J. (2022). A critical review of the ultrastructure, mechanics and modelling of flax fibres and their defects. *Progress in Materials Science*, 124(July 2020), Article 100851. <https://doi.org/10.1016/j.pmatsci.2021.100851>
- Rihouey, C., Paynel, F., Gorshkova, T., & Morvan, C. (2017). Flax fibers: Assessing the non-cellulosic polysaccharides and an approach to supramolecular design of the cell wall. *Cellulose*, 24(5), 1985–2001. <https://doi.org/10.1007/s10570-017-1246-5>
- Shafizadeh, F., & Lai, Y. Z. (1972). Thermal degradation of 1,6-anhydro-beta-D-glucopyranose. *The Journal of Organic Chemistry*, 37(2), 278–284.
- Shah, D. U. (2013). Developing plant fibre composites for structural applications by optimising composite parameters: A critical review. *Journal of Materials Science*, 48(18), 6083–6107. <https://doi.org/10.1007/s10853-013-7458-7>
- Siniscalco, D., Arnould, O., Bourmaud, A., Le Duigou, A., & Baley, C. (2018a). Corrigendum to “Monitoring temperature effects on flax cell-wall mechanical properties within a composite material using AFM” [Polym. Test. 69 (2018) 91–99]. *Polymer Testing*, 72, 439. <https://doi.org/10.1016/j.polymeresting.2018.10.009>
- Siniscalco, D., Arnould, O., Bourmaud, A., Le Duigou, A., & Baley, C. (2018b). Monitoring temperature effects on flax cell-wall mechanical properties within a composite material using AFM. *Polymer Testing*, 69, 91–99. <https://doi.org/10.1016/j.polymeresting.2018.05.009>
- Snegireva, A. V., Ageeva, M. V., Amenitskii, S. I., Chernova, T. E., Ebskamp, M., & Gorshkova, T. A. (2010). Intrusive growth of sclerenchyma fibers. *Russian Journal of Plant Physiology*, 57(3), 342–355. <https://doi.org/10.1134/S1021443710030052>
- Stanzl-Tscheegg, S., Beikircher, W., & Loidl, D. (2009). Comparison of mechanical properties of thermally modified wood at growth ring and cell wall level by means of instrumented indentation tests. *Holzforschung*, 63(4), 443–448. <https://doi.org/10.1515/HF.2009.085>
- Tejado, A., Peña, C., Labidi, J., Echeverría, J. M., & Mondragon, I. (2007). Physico-chemical characterization of lignins from different sources for use in phenol-formaldehyde resin synthesis. *Bioresource Technology*, 98(8), 1655–1663. <https://doi.org/10.1016/j.biortech.2006.05.042>
- Thomason, J. L., & Rudeiros-Fernández, J. L. (2021). Thermal degradation behaviour of natural fibres at thermoplastic composite processing temperatures. *Polymer Degradation and Stability*, 188, Article 109594. <https://doi.org/10.1016/j.polymerdegradstab.2021.109594>
- Wada, M., Hori, R., Kim, U.-J., & Sasaki, S. (2010). X-ray diffraction study on the thermal expansion behavior of cellulose I β and its high-temperature phase. *Polymer Degradation and Stability*, 95(8), 1330–1334. <https://doi.org/10.1016/j.polymerdegradstab.2010.01.034>
- Yin, Y., Berglund, L., & Salmén, L. (2011). Effect of steam treatment on the properties of wood cell walls. *Biomacromolecules*, 12(1), 194–202. <https://doi.org/10.1021/bm101144m>
- Yu, J., Sun, L., Ma, C., Qiao, Y., & Yao, H. (2016). Thermal degradation of PVC: A review. *Waste Management*, 48(September), 300–314. <https://doi.org/10.1016/j.wasman.2015.11.041>
- Yu, Y., Fei, B., Wang, H., & Tian, G. (2011). Longitudinal mechanical properties of cell wall of Masson pine (*Pinus massoniana* Lamb) as related to moisture content: A nanoindentation study. *Holzforschung*, 65(1), 121–126. <https://doi.org/10.1515/hf.2011.014>
- Zickler, G. A., Schöberl, T., & Paris, O. (2006). Mechanical properties of pyrolysed wood: A nanoindentation study. *Philosophical Magazine*, 86(10), 1373–1386. <https://doi.org/10.1080/14786430500431390>
- Zollfrank, C., & Fromm, J. (2009). Ultrastructural development of the softwood cell wall during pyrolysis. *Holzforschung*, 63(2), 248–253. <https://doi.org/10.1515/HF.2009.031>